Cellular preservation of excysting developmental stages of new eukaryotes from the early Ediacaran Weng'an Biota

Emma N.U. Landon [a], Peng-Ju Liu [b], Zong-Jun Yin [c] *, Wei-Chen Sun [c, d], Xiao-Dong Shang [b], Philip C.J. Donoghue [a] *

[a] School of Earth Sciences, University of Bristol, Life Sciences Building, Tyndall Avenue, Bristol BS8 1TQ, UK

[b] Institute of Geology, Chinese Academy of Geological Sciences, Beijing 100037, China

[c] State Key Laboratory of Palaeobiology and Stratigraphy, Nanjing Institute of Geology and Palaeontology and Center for Excellence in Life and Paleoenvironment, Chinese Academy of Sciences, Nanjing 210008, China

[d] University of Science and Technology of China, Hefei 230026, China

* Corresponding authors. *E-mail addresses*: zjyin@nigpas.ac.cn, Phil.Donoghue@bristol.ac.uk

Abstract

The Ediacaran Weng'an Biota provides a unique window on marine diversity during the interval in which the fundamental animal body plans were being established. Here we describe a previously unreported component of the assemblage, millimeter-scale encysted spheres that exhibit a characteristic but simple slit-shaped excystment mechanism (*Sporosphaera guizhouensis* n. gen. n. sp.), reminiscent of acritarchs. The cysts contain a large inner body or numerous small discrete membrane-bounded bodies. It is possible that the inner bodies represent disaggregated cells of a multicellular body, like an embryo, but there is no evidence to support this interpretation and the occurrence of the excystment structure is not readily compatible with an embryo interpretation. Rather, we interpret the encysted organisms as multicellular stages within the lifecycle of otherwise probably unicellular eukaryotes.

The developmental mode exhibited by *Sporosphaera*, incorporating a resting stage, implies an adaptation to adverse environmental conditions. This parallels the appearance of Large Ornamented Ediacaran Microfossils (LOEMs) which have been interpreted as diapause stages in the embryology of early animals. *Sporosphaera* is distinct from LOEMs by ornamentation instead of size, which may implicate that not all LOEMs are animal embryos, if any.

Keywords: Weng'an Biota; Ediacaran; acritarch; eukaryote; excystment mechanism

1. Introduction

The 609 million-year-old Weng'an Biota (Zhou et al., 2017) is among the most exquisite of fossil lagerstätte (Xiao et al., 2014; Cunningham et al., 2017b), preserving in calcium phosphate the three-dimensional remains of unicellular and multicellular organisms to a subcellular (Hagadorn et al., 2006) and even organelle level of fidelity (Yin et al., 2017). However, the great significance of the exceptionally preserved Weng'an biota is rooted in its temporal context, by providing a unique window to look at marine biodiversity long before the appearance of uncontroversial animal fossils but within the interval of geological time in which the fundamental lineages of bilaterian phyla were estimated to have diverged base on molecular clocks (dos Reis et al., 2015; Cunningham et al., 2017a).

The Weng'an Biota is dominated by millimeter to submillimeter scale embryo-like remains attributed to *Megasphaera*, *Parapandorina*, *Megaclonophycus*, and *Tianzhushania.* They have been the focus of research because of their debated animal affinity (Xiao et al., 1998, 2007; Hagadorn et al., 2006; Bailey et al., 2007; Chen et al., 2014; Zhang and Pratt, 2014; Yin et al., 2016), leaving the remaining fossils in the Weng'an biota largely understudied. Here we describe a previously unreported component of the Weng'an Biota encompassing millimeter-scale encysted spheres that exhibit a characteristic but simple slit-shaped excystment mechanism, reminiscent of acritarch cysts, with evidence of a multicellular structure. We establish a new genus and species, *Sporosphaera guizhouensis* n. gen. n. sp. based on the specimens

presented herein and explore the taphonomy, biology, affinity, evolutionary and environmental implications of these fossils.

2. Materials and methods

The specimens were recovered from the Upper Phosphorites of the Doushantuo Formation in the '54 Quarry', Weng'an County, Guizhou Province, Southwest China (Cunningham et al., 2017b). Rock samples were subjected to dissolution in 8–10% acetic acid, dissolving the calcium carbonate cement and matrix to leave an insoluble residue of phosphates, silicates and pyrite. This residue was sorted manually under a binocular stereomicroscope. Selected specimens were subjected to microtomography at the TOMCAT (X02DA) beamline of the Swiss Light Source (SLS), Paul Scherrer Institute (Villigen, Switzerland) or the BM5 beamline of the European Synchrotron Radiation Facility (ESRF, Grenoble, France). X-Ray projections were obtained at 1501 or 1800 stepwise increments through a 180º rotation of the specimen, at beam energies ranging from 19–21 KeV, exposure times of 110–1000 milliseconds and using scintillators composed of lutetium, aluminium and garnet. The X-Ray projections were rearranged into dark- and flatfield-corrected sinograms, after which they were reconstructed using a gridding procedure and a highly optimized routine based on the Fourier transform method (Marone et al., 2010). The resulting datasets of reconstructed tomographic slices have a voxel resolution of 0.74 µm (10× objective) and 0.36 µm (20× objective) at SLS, or 0.75 µm (10× objective) at ESRF. The studied specimens are deposited in the Nanjing Institute of Geology and Palaeontology, Chinese Academy of Sciences. Following best practice for digital morphology (Davies et al., 2017), our tomographic datasets and models are available from http://dx.doi.org/10.5523/bris.xxxx and Geobiodiversity Database at http://www.geobiodiversity.com.

3. Results

3.1. External morphology

The fossils are all spheroidal, approximately 1 mm in diameter, smooth, unornamented and otherwise featureless apart from a shallow ambital slit that varies between 50–60 μm in depth and 158–445 μm in width, representing half to two-thirds of the circumference at its greatest extent (Figs. 1–3). The radial angle relative to the margins of the slit varies between 7.4º (Fig. 1) and 46.7º (Fig. 2) in different specimens. The slits with small radial angles look like narrow, arcuate troughs when observed from the surface (Fig. 1A-G, K-Q, T, V), while those with broader radial angles are rounded in outline, and the resulting trough does not extend far (no more than 60 μm in depth) with a rounded base (Fig. 2A-C, F-H). In some specimens, the original cyst walls are not preserved, or were lost through laboratory processing (Fig. 2A-C, F-H), and so there is no preserved structure at the slit margins. In contrast, the specimen with the broadest slit (Fig. 2K-N) preserves the slit margins of the cyst curled inward (Fig. 2K, L) and a crescentic mass of small spheres, cemented by a phosphatic matrix, protruding from the slit (Fig. 2K-N). A number of these small spheres appear to have been preserved while being released to the external environment (Fig. 2L, M). The retention of the crescentic mass of small spheres with this specimen suggests that it may have possessed an outer envelope that has not been preserved, preventing the release of the small spheres.

3.2. Internal structure

Specimens can be attributed to three broad categories of internal preservation. In general, most specimens preserve no discernable biological structure (Fig. 3) and most of the interior volume of the fossils is comprised of a granular matrix (grains approximately 2 μm in diameter), permeated with micrometer scale pores and cross-cut by fine cracks (Fig. 3A-C), or internally they exhibit anastomosing layers of void-filling linings (e.g., Fig. 3D-F). The specimens are principally composed of calcium phosphate, but there is some subtle variation in composition as reflected by differences in contrast and, therefore, X-Ray attenuation, which reflects the atomic number of the material. Some voids are filled with a high contrast, low attenuation phase of calcite or dolomite.

More rarely, distinct inner-bodies are preserved that vary in size and number (Figs. 1E-H, O-R, T-W, 2C, H, L, M). A few specimens contain only one large internal body (e.g., Fig. 2A-J). Some of these are irregular but the most distinct is approximately spherical (Fig. 2C-E, H-J; shortest diameter 265.4 μm, longest diameter 290.6 μm). The large inner body is either filled with void-filling cement (Fig. 2C-E) or else exhibits a distinct outer fine-grained mantle and void-filling core (Fig. 2H-J). In such circumstances, the rest of the fossil is comprised of a porous mineral phase in which the texture is dominated by small voids or dark mineral microspheres, all of approximately the same diameter (~2 μm) (Fig. 2I, J). The inner body is slightly off-center in one specimen (Fig. 2H-J), and it is about 30% of the diameter of the whole specimen. It has a distinct mineralogy, with an outer dense layer, approximately half its radius (some pores) and an equally distinct bright, low-attenuating core that may be a void-fill (Fig. 2H-J). Another specimen also includes an inner body of approximately the same relative volume, but it is positioned off-center and is distinguished by more void-filling cement (Fig. 2C-E). The surrounding mineral is more compact, with fewer, larger pores associated with secondary void-filling mineralization (Fig. 2D, E).

A number of specimens (Fig. 1) preserve numerous (20–60) small spheroidal vesicles disseminated discretely throughout their interior, ranging in size from 25 to 121 μm in diameter, with a membrane thickness of 3.9 to 5.3 μm. The vesicle membrane itself has a distinct, homogeneous fabric and X-Ray attenuation profile while the outer mineral matrix is more variable (Fig. 1H-J, R, S, U, W-Y). The vesicles are usually at least partially or else completely filled with a bright (low attenuation) mineral phase that is largely homogeneous and appears to represent a late void-filling cement (Fig. 1R, S, U, W-Y); this interpretation is supported by the observation that in some specimens, some vesicles are empty (Fig. 1I, J, S, X). High resolution imaging reveals the vesicle membranes to have been among the first structures being mineralized since they have been preserved as a dark mineral phase with a much higher X-Ray attenuation than the matrix (Fig. 1I, J, S, X, Y). Many, but

not all of the specimens preserve evidence of a distinct surface layer as a more highly attenuating mineral phase (e.g., Fig. 3D-F).

4. Discussion

4.1. Distinguishing geology from biology

Differences in the structure of the fossils reflect a combination of geological and biological factors. Differences in the number of internal structures could reflect differences in the biological affinity of the fossils, but the consistency in size, shape, and the nature of the slit suggests that they represent a taxonomically coherent assemblage. The fossils differ principally in the longitudinal extent and breadth of the slit, which we interpret to reflect developmental differences. The fossils also differ significantly in terms of their internal structures, which we interpret principally as a consequence of biostratinomy.

The biostratinomy of the Weng'an Biota has been considered previously (Cunningham et al., 2012; Schiffbauer et al., 2012; Yin et al., 2014, 2017), discriminating early phases of mineralization which preserve biological structure from later void-filling mineralization and late diagenetic mineral phases. Mineral phases preserving biological structure are invariably microcrystalline and randomly oriented, reflecting growth on and within an organic template; later phases unrelated to the original biological structure are usually more coarsely crystalline and polarized, reflecting centripetal and centrifugal void-filling growth relative to existing mineral substrates (Cunningham et al., 2012).

The anastomosing palisade mineral structure of many of the fossils is compatible with void-filling after most of the original internal biological structure had decayed away. Most of the fossils otherwise exhibit a structureless and homogeneous interior which reflects mineralization of a structureless, extensively decayed cyst interior (Fig. 3). The low contrast, low-attenuation mineral microspheres that characterize the mineralization of the interior of some cysts (e.g., Fig. 2H-J), is characteristic of mineral-replicated biological structure in other Weng'an fossils

(Cunningham et al., 2012). Their consistent shape and distribution is compatible with preservation of original biological structure, as component cells as in *Megaclonophycus* (Cunningham et al., 2012), or as small lipid droplets (Hagadorn et al., 2006; Raff et al., 2006). The microspheres are invariably enveloped by centrifugally arranged layers of a brighter mineral phase (Fig. 2I, J; refer to Yin et al., 2017, fig. 1d, h); some of the spheres are unmineralized, reflecting non-preservation of structures that remained physically intact while the void-filling process proceeded.

The two classes of larger internal structures exhibit compatible diagenetic records; the membranes of the small vesicles and the outer layer of the large singular structures, are both characterized by a dark, low X-Ray attenuation mineral phase, compatible with early mineralization of original unmineralized biological structure, while their lumens are filled with a bright, high low X-Ray attenuation mineral phase, compatible with later void-filling mineralization in Weng'an fossils (Cunningham et al., 2012). This interpretation is corroborated by the occurrence of empty lumens in subsets of the small vesicles in some specimens (e.g., Fig. 1X, Y). The cyst walls themselves are often characterized by a thin bright, high X-Ray attenuation mineral phase, indicating that the cyst wall itself is preserved through late, void-filling diagenetic mineralization, and that the originally unmineralized cyst wall remained structurally intact while the interior was mineralized, later lost through decay. This mirrors the preservation of cell membranes associated with the embryo-like fossils attributed variably to *Tianzhushania*, *Megasphaera*, *Parapandorina*, and *Megaclonophycus* (Cunningham et al., 2012).

Thus, we discriminate the cyst walls, the large singular and numerous smaller internal structures, and the microspheres as original biological structures worthy of interpretation.

4.2. Palaeobiology: large, singular internal structures

The large, singular internal structures of the specimens shown in Fig. 2A and F exhibit a strong resemblance, in terms of size and shape, as well as positional and preservational variation, to the 'large intracellular structures' described from the

embryo-like fossils *Tianzhushania* and *Spiralicellula*, from the same deposit (Hagadorn et al., 2006; Huldtgren et al., 2011; Schiffbauer et al., 2012; Yin et al., 2017). These structures were originally interpreted as 'nuclei, spindle bundles, or other organelles' (Hagadorn et al., 2006), constrained as nuclei based on consistency of size, shape and topology, subsequently dismissed as degraded cytoplasmic remains (Schiffbauer et al., 2012; Xiao et al., 2012, 2014; Pang et al., 2013) based principally on incredulity that nuclei could be fossilized (Pang et al., 2013). The nucleus interpretation of these structures has since been corroborated based on quantitative characterization of the volumetric relationship between the 'large internal structures' and their host cells, across successive rounds of palintomy represented in the fossil assemblage (Yin et al., 2017). The large internal structures exhibit differences in the predominant mode of preservation in *Sporosphaera* versus *Tianzhushania* and *Spiralicellula*; in the former, the border is characterized by early mineralization of a biological substrate, whereas in the latter, the border is typically characterized by later diagenetic void-filling mineralization (Schiffbauer et al., 2012). However, the large internal structures exhibit an overlapping range of preservational modes such that in *Sporosphaera* the structure has an irregular border and is characterized by void-filling mineralization (e.g., Fig. 2D, E), presumably reflecting preservation of decayed remains; in *Tianzhushania* and *Spiralicellula*, an organic outer membrane can be preserved (Yin et al., 2017). The large internal structures in *Sporosphaera* also exhibit variation in position within the cyst, mirroring that of the nuclei in *Tianzhushania* and *Spiralicellula* where this might reflect the *in vivo* position of their nucleus, but also co-varies with the preservational state of the nucleus itself and, therefore, must reflect the role of intracellular degradation. The most poorly preserved large internal structure in *Sporosphaera* is positioned away from the center of the cyst (Fig. 2C).

Based on similarity in preservation, size and position to the large intracellular structures in *Tianzhushania* and *Spiralicellula*, the large, singular internal structures in *Sporosphaera* can also be interpreted as preserved nuclei. However, it remains possible that the similarity does not extend beyond size and preservational mode, and they could be the shrunken and decayed remains of a cluster of cells.

4.3. Palaeobiology: small vesicles

The small vesicles in the specimens shown in Fig. 1 do not compare well to the larger, singular internal structures, either in terms of their preservation or their size, number and position within the cyst. Both the '*Parapandorina*' and '*Megaclonophycus*' stages of *Tianzhushania* preserve structures that are comparable to the small vesicles; these structures are interpreted as lipid vesicles or yolk granules in 'Parapandorina' stages (Hagadorn et al., 2006; Cunningham et al., 2012), and as the component cells in 'Megaclonophycus' stages (Cunningham et al., 2012). In both cases, the structures are far more numerous and, consequently, densely packed than are the vesicles in *Sporosphaera*. The style of preservation exhibited by the vesicles in *Sporosphaera* is most comparable to that seen in at least some specimens of 'Megaclonophycus' stages (e.g., Cunningham et al., 2012), where the membrane is preserved by dark, low attenuation dense mineral phase, indicative of early mineralization, replicating original biological structure. This likely reflects simply that the membranes have a similar preservational style in *Sporosphaera* and '*Megaclonophycus*' stages of *Tianzhushania*, providing support for the interpretation of the vesicles in *Sporosphaera* as component cells; it is difficult to conceive a credible alternative biological interpretation.

4.4. Development

The internal vesicles of *Sporosphaera* look very similar to the small cells of '*Megaclonophycus*' stages of *Tianzhushania*. Both *Sporosphaera* and *Tianzhushania* are recovered from the same deposit and share similar morphology and size. These superficial similarities between them may lead to an argument that they represent different development stages of the same taxon or several closely related taxa. However, it is difficult to reconcile the *Sporosphaera* with the development pattern of *Megasphaera–Parapandorina–Megaclonophycus* complex (or *Tianzhushania* complex), because no slit or similar structures have been observed in any *Tianzhushania* specimens, and no evidence indicates that *Sporosphaera* possesses an

ornamented envelope similar to that of *Tianzhushania*. Following the interpretation of the small vesicles in *Sporosphaera* as cell membranes, they might either represent individuals in an essentially unicellular organism, or else the disaggregated cells of a multicellular stage in the lifecycle of an otherwise unicellular or multicellular organism. Diverse unicellular eukaryotes exhibit a multicellular stage in otherwise unicellular organisms, including propagules of mesomycetozoans, sporangia of slime molds, and green algae. Alternatively, taphonomy experiments have shown that multicellular embryos of multicellular organisms can disaggregate to yield loose assemblages of individual cells (Raff et al., 2006). The comparatively small number of vesicles in any one *Sporosphaera* and, critically, their comparatively small collective volume relative to that of the host cyst, speaks against their interpretation as the disaggregated components of a multicellular embryo. The slit in *Sporosphaera* is not incompatible with an embryo-interpretation; for example, animals that mechanically escape their fertilization envelope often leave via a simple slit-shaped rupture. However, this is a feature of embryos comprised of hundreds of cells; animal embryos comprised of small numbers of cells tend to maintain cell adhesion post mortem (Raff et al., 2006) and in most other eukaryotes that have an embryonic stage, the component cells aggregate as a consequence of incomplete cytoplasmic division (Green et al., 1981; Rensing, 2016; Cunningham et al., 2017b), a feature also seen in sponges (Degnan et al., 2015). Neither is seen in *Sporosphaera* and there is no evidence that the cells are ever clustered. Thus, we conclude that these multicelled stages of *Sporosphaera* do not represent embryos but, rather, a stage in the life cycle of component individual unicellular organisms.

Obviously, the extent of the slit, in terms of its width, is not correlated with the number of internal bodies that the specimen contains, since specimens with both very broad and narrow ambital slits contain numerous small cells. However, the observation that the width and shape of the slit varies from narrow and acute to broad and rounded in different specimens leads to interpretation as polarity in a developmental process, perhaps associated with the progressive maturation and release of the cells. However, it is difficult to rationalize the specimens with single

large internal bodies and broad slits (Fig. 2A-J) in this developmental pattern. That said, these two specimens are taphonomic outliers, preserved as inner casts, suggesting that the original cysts decayed out and the original width of the slits is difficult to constrain. Certainly a pattern of reduction from an encysted mother cell to numerous spores is compatible with vegetative phases in the life cycle of numerous unicellular eukaryotes (Mendoza et al., 2002; Schaap, 2012); no viable interpretation is compatible with a metazoan affinity.

4.5. Evolutionary and environmental interpretations

While the affinity of *Sporosphaera* is difficult to constrain beyond that of a unicellular eukaryote, what can be gleaned of its life cycle, undergoing episodic encystment, is informative on the nature of Ediacaran marine environments. Cohen et al. (2009) have observed that large ornamented Ediacaran 'acritarch' cysts are the recalcitrant remains of metazoan diapause embryos, an adaptation to widespread anoxia of marine bottom conditions. Their argument is based on the observation that such cysts, including *Tianzhushania*, can be demonstrated to have contained embryo-like fossils (Yin et al., 2007), are comparable to modern diapause cysts in terms of their size, shape, ornamentation, and ultrastructure, and disappear from palynological assemblages in association with the oxygenation of continental shelves. It is now known that temporal and spatial variation in the oxygenation of continental shelf bottom waters continued into the Cambrian (Bowyer, 2017) and, though the class of large ornamented microfossils interpreted as diapause stages by Cohen et al. (2009) may well be limited to the Ediacaran, this life history strategy continued into the Cambrian (Yin et al., 2018). *Sporosphaera*, too, appears to further nuance this general hypothesis in demonstrating that unornamented equivalents of the large ornamented Ediacaran acritarchs also represent encysted developmental stages, albeit not of metazoans. This suggests that the prevalence of widespread marine anoxia impacted not only on the life history strategy of early metazoans, but also on eukaryotes more generally.

5. Conclusions

The fossils show similarity to features of the *Tianzhushania* complex, but they are clearly distinct. Some have argued that all of the embryo-like fossils in the Weng'an Biota can effectively be synonymized, but the similarity and differences exhibited by these fossils evidence a greater diversity of embryo-like fossils within the Weng'an Biota. That they are consistently preserved in cysts suggests that they may represent a resting stage within a broader life cycle, perhaps an adaptation for the temporal and spatial variability of Ediacaran shallow marine environments.

6. Systematic Palaeontology

Kingdom Eukaryota
Phylum Incertae Sedis

Genus *Sporosphaera* n. gen.

Etymology: The name is derived from Latin and named in reference to the spherical morphology of the fossils, and the ability to produce spores.
Type species: *Sporosphaera guizhouensis* n. gen. n. sp., by monotype.
Diagnosis: As for the type species.
Occurrence: '54 Quarry' in Weng'an County, Guizhou Province, Southwest China; Doushantuo Formation, Upper Phosphorite Member, early Ediacaran.

Sporosphaera guizhouensis n. sp.
(Fig. 1A-H)

Etymology: Reference to Guizhou Province, where the fossils were found.
Holotype: Reg. no. NIGP 170566 (Fig. 1A-H). The holotype has been deposited in the collection of Nanjing Institute of Geology and Palaeontology (NIGP).

Diagnosis: A spheroidal unornamented cyst, 1 mm diameter, with an ambital excystment structure. Contains small, discrete, spheroidal membranes.

Occurrence: '54 Quarry' in Weng'an County, Guizhou Province, Southwest China; Upper Phosphorite Member, Doushantuo Formation, early Ediacaran. More than 500 specimens in total have been discovered.

Description: A spheroidal unornamented cyst, 1 mm diameter, with an ambital excystment structure that varies between 50–60 μm in depth and 158–445 μm in width, representing half to two-thirds of the circumference at its greatest extent. The extreme margins of the excystment structure are rounded in outline and the resulting trough is shallow and has a rounded base. The radial angle relative to the margins of the excystment structure varies between 7.4º and 46.7º.

In general, most of the interior volume of the fossils is comprised of a granular matrix, permeated with micrometer scale pores and cross-cut by fine cracks. Most specimens preserve no discernable biological structure; internally they are homogeneous or exhibit anastomosing layers of void-filling cement. A smaller number of specimens are generally homogeneous but preserve a distinct clotted fabric of high and low attenuating mineral phases at the margins of the slit in the surface of the fossil, and in some this clotted fabric comprises the entire volume of the specimen. The best-preserved specimens contain between one and forty spheroidal internal structures, which vary between 25 and 290 μm in diameter.

Remarks: The single large inner body preserved in some specimens is reminiscent of the structures interpreted as nuclei in the embryo-like fossils *Tianzhushania* and *Spiralicellula* (Yin et al., 2017). The smaller spheroidal structures disseminated throughout the interior of some other specimens resemble structures in the '*Parapandorina*' stage of *Tianzhushania* that have been interpreted as lipid droplets, possibly yolk granules (Hagadorn et al., 2006; Cunningham et al., 2012). These structures also bear some resemblance to the '*Megaclonophycus*' stage of the *Tianzhushania* complex, although in '*Megaclonophycus*' stage the structures are interpreted as cells and are much more closely packed than the structures in

Sporosphaera guizhouensis, which comprise far less of the internal volume and do not touch.

Acknowledgements

We are grateful to prof. Chuan-Ming Zhou and the anonymous reviewer for their critical comments and suggestions. This research was funded by NERC Thematic Grant NE/P013678/1 to PCJD and ZJY, a Royal Society Newton Advanced Fellowship to ZJY and PCJD, a NERC GW4+ DTP Studentship to ENUL, National Natural Science Foundation of China (41672013, 41572016) to ZJY and PJL, and the Youth Innovation Promotion Association of the Chinese Academy of Sciences (2017360) to ZJY.

References

Bailey, J.V., Joye, S.B., Kalanetra, K.M., Flood, B.E., Corsetti, F.A., 2007, Evidence of giant sulphur bacteria in Neoproterozoic phosphorites. Nature 445 (7124), 198-201.

Bowyer, F., Wood, R.A., Poulton, S.W., 2017. Controls on the evolution of Ediacaran metazoan ecosystems: A redox perspective. Geobiology 15, 516-551.

Chen, L., Xiao, S.H., Pang, K., Zhou, C.M., Yuan, X.L., 2014, Cell differentiation and germ-soma separation in Ediacaran animal embryo-like fossils. Nature 516 (7530), 238-241.

Cohen, P.A., Knoll, A.H., Kodner, R.B., 2009. Large spinose microfossils in Ediacaran rocks as resting stages of early animals. Proceedings of the National Academy of Sciences of the United States of America 106 (16), 6519-6524.

Cunningham, J.A., Thomas, C.W., Bengtson, S., Kearns, S.L., Xiao, S.H., Marone, F., Stampanoni, M., Donoghue, P.C.J., 2012. Distinguishing geology from biology in the Ediacaran Doushantuo biota relaxes constraints on the timing of the origin of bilaterians. Proceedings of the Royal Society B: Biological Sciences 279 (1737), 2369-2376.

Cunningham, J.A., Liu, A.G., Bengtson, S., Donoghue, P.C.J., 2017a. The origin of animals: Can molecular clocks and the fossil record be reconciled? Bioessays 39 (1), doi: 10.1002/bies.201600120.

Cunningham, J.A., Vargas, K., Yin, Z.J, Bengtson, S., Donoghue, P.C.J., 2017b. The Weng'an Biota (Doushantuo Formation): an Ediacaran window on soft-bodied and multicellular microorganisms. Journal of the Geological Society 174, 793-802.

Davies, T.G., Rahman, I.A., Lautenschlager, S., Cunningham, J.A., Asher, R.J., Barrett, P.M., Bates, K.T., Bengtson, S., Benson, R.B.J., Boyer, D.M., Braga, J., Bright, J.A., Claessens, L.P.A.M., Cox, P.G., Dong, X.P., Evans, A.R., Falkingham, P.L., Friedman, M., Garwood, R.J., Goswami, A., Hutchinson, J.R., Jeffery, N.S., Johanson, Z., Lebrun, R., Martinez-Perez, C., Marugan-Lobon, J., O'Higgins, P.M., Metscher, B., Orliac, M., Rowe, T.B., Rucklin, M., Sanchez-Villagra, M.R., Shubin, N.H., Smith, S.Y., Starck, J.M., Stringer, C., Summers, A.P., Sutton, M.D., Walsh, S.A., Weisbecker, V., Witmer, L.M., Wroe, S., Yin, Z.J, Rayfield, E.J., Donoghue, P.C.J., 2017. Open data and digital morphology. Proceedings of the Royal Society B: Biological Sciences 284 (1852), doi: 10.1098/rspb.2017.0194.

Degnan, B.M., Adamska, M., Richards, G.S., Larroux, C., Leininger, S., Bergum, B., Calcino, A., Taylor, K., Nakanishi, N., Degnan, S.M., 2015. Porifera. In: Wanninger, A. (Ed.), Evolutionary Developmental Biology of Invertebrates 1: Introduction, Non-bilateria, Acoelomorpha, Xenoturbella, Chaetognatha. Springer-Verlag, Wien, pp. 65-106.

dos Reis, M., Thawornwattana, Y., Angelis, K., Telford, M.J., Donoghue, P.C.J., Yang, Z.H., 2015. Uncertainty in the timing of origin of animals and the limits of precision in molecular timescales. Current Biology 25 (22), 2939-2950.

Green, K.J., Viamontes, G.I., Kirk, D.L., 1981. Mechanism of formation, ultrastructure, and function of the cytoplasmic bridge system during morphogenesis in Volvox. Journal of Cell Biology 91, 756-769.

Hagadorn, J.W., Xiao, S.H., Donoghue, P.C.J., Bengtson, S., Gostling, N.J., Pawlowska, M., Raff, E.C., Raff, R.A., Turner, F.R., Yin, C.Y., Zhou, C.M., Yuan, X.L., McFeely, M.B., Stampanoni, M., Nealson, K.H., 2006. Cellular and subcellular structure of neoproterozoic animal embryos. Science 314 (5797), 291-294.

Huldtgren, T., Cunningham, J.A., Yin, C.Y., Stampanoni, M., Marone, F., Donoghue, P.C.J., Bengtson, S., 2011. Fossilized nuclei and germination structures identify Ediacaran "animal embryos" as encysting protists. Science 334 (6063), 1696-1699.

Marone, F., Münch, B., Stampanoni, M., 2010. Fast reconstruction algorithm dealing with tomography artifacts. Proceedings of SPIE 7804, 780410, doi: 10.1117/12.859703.

Mendoza, L., Taylor, J.W., Ajello, L., 2002. The class Mesomycetozoea: a heterogeneous group of microorganisms at the animal-fungal boundary. Annual Review of Microbiology 56, 315-344.

Pang, K., Tang, Q., Schiffbauer, J.D., Yao, J., Yuan, X.L., Wan, B., Chen, L., Ou, Z.J., Xiao, S.H., 2013. The nature and origin of nucleus-like intracellular inclusions in Paleoproterozoic eukaryote microfossils. Geobiology 11 (6), 499-510.

Raff, E.C., Villinski, J.T., Turner, F.R., Donoghue, P.C.J., Raff, R.A., 2006. Experimental taphonomy shows the feasibility of fossil embryos. Proceedings of the National Academy of Sciences of the United States of America 103 (15), 5846-5851.

Rensing, S.A., 2016. (Why) Does evolution favour embryogenesis? Trends in Plant Science 21 (7), 562-573.

Schaap, P., 2012. Evolutionary crossroads in developmental biology: Dictyostelium discoideum. Development 138, 387-396.

Schiffbauer, J.D., Xiao, S.H., Sen Sharma, K., Wang, G., 2012. The origin of intracellular structures in Ediacaran metazoan embryos. Geology 40 (3), 223-226.

Xiao, S.H., Zhang, Y., Knoll, A.H., 1998, Three-dimensional preservation of algae and animal embryos in a Neoproterozoic phosphorite. Nature 391 (6667), 553-558.

Xiao, S.H., Hagadorn, J.W., Zhou, C.M., Yuan, X.L., 2007, Rare helical spheroidal fossils from the Doushantuo Lagerstatte: Ediacaran animal embryos come of age? Geology 35 (2), 115-118.

Xiao, S.H., Knoll, A.H., Schiffbauer, J.D., Zhou, C.M., Yuan, X.L., 2012. Comment on "Fossilized nuclei and germination structures identify Ediacaran 'animal embryos' as encysting protists". Science 335 (6073), 1169-c, doi: 10.1126/science.1218814.

Xiao, S.H., Muscente, A.D., Chen, L., Zhou, C.M., Schiffbauer, J.D., Wood, A.D., Polys, N.F., Yuan, X.L., 2014. The Weng'an biota and the Ediacaran radiation of multicellular eukaryotes. National Science Review 1 (4), 498-520.

Yin, L.M., Zhu, M.Y., Knoll, A.H., Yuan, X.L., Zhang, J.M., Hu, J., 2007. Doushantuo embryos preserved inside diapause egg cysts. Nature 446 (7136), 661-663.

Yin, Z.J., Liu, P.J., Li, G., Tafforeau, P., Zhu, M.Y., 2014. Biological and taphonomic implications of Ediacaran fossil embryos undergoing cytokinesis. Gondwana Research 25 (3), 1019-1026.

Yin, Z.J., Zhu, M.Y., Bottjer, D.J., Zhao, F.C., Tafforeau, P., 2016. Meroblastic cleavage identifies some Ediacaran Doushantuo (China) embryo-like fossils as metazoans. Geology 44 (9), 735-738.

Yin, Z.J., Cunningham, J.A., Vargas, K., Bengtson, S., Zhu, M.Y., Donoghue, P.C.J., 2017, Nuclei and nucleoli in embryo-like fossils from the Ediacaran Weng'an Biota. Precambrian Research 301, 145-151.

Yin, Z.J., Zhao, D.D., Pan, B., Zhao, F.C., Zeng, H., Li, G.X., Bottjer, D.J., Zhu, M.Y., 2018. Early Cambrian animal diapause embryos revealed by X-ray tomography. Geology 46, 387-390.

Zhang, X.G., Pratt, B.R., 2014. Possible algal origin and life cycle of Ddiacaran Doushantuo microfossils with dextral spiral structure. Journal of Paleontology 88 (1), 92-98.

Zhou, C.M., Li, X.H., Xiao, S.H., Lan, Z.W., Ouyang, Q., Guan, C.G., Chen, Z., 2017. A new SIMS zircon U-Pb date from the Ediacaran Doushantuo Formation: age constraint on the Weng'an biota. Geological Magazine 154 (6), 1193-1201.

Figure captions

Fig. 1. Volume renders of *Sporosphaera* fossils with narrow slits. (A-D) 3-D surface renderings of the specimen NIGP 170566 from different view angles, showing the narrow slit. (E-G) Transparent models of (A-C), respectively, showing distribution of small inner bodies (yellow spheres). (H) An orthoslice of (D), showing inner bodies. (I, J) Close-up views of inner bodies from (H), showing preservation detail. (K-N) 3-D surface renderings of the specimen WA_B3_H03E from different view angles, showing the narrow slit. (O-Q) Transparent models of (K-M), respectively, showing distribution of small inner bodies (pink spheres). (R) An orthoslice of (N). (S) A close-up view of (R), displaying inner bodies. (T, V) Surface renderings of specimen ZY1216_21 and ZY1709_11. (U, W) Orthoslices of (T, V), respectively. (X, Y) Close-up views of (T, V), respectively, showing the inner bodies.

Fig. 2. Volume renders and SEM images of *Sporosphaera* fossils with broad slits. (A, B) 3-D surface renderings of specimen ZY1216_13. (C) Orthoslice of (B), showing a large inner body. (D, E) Close-up views of the inner body shown in (C) from different depth. (F, G) 3-D surface renderings of specimen ZY1216_20. (H) Orthoslice of (G), showing a large inner body. (I, J) Close-up views of the inner body shown in (H) from different depth; the dotted circles in (J) indicate the boundaries of the mantle and core.

(K, L) SEM images of specimen WA_B1_D02. (M, N) Close-up views of the center area in (L), showing details of the small spheres and slit margins.

Fig. 3. Volume renders of *Sporosphaera* specimens without internal biological structures. (A, B) 3-D surface renderings of specimen ZY1709_05. (C) Orthoslices of ZY1709_05, showing internal diagenetic structures. (D, E) 3-D surface renderings of specimen ZY1709_15. (F) Orthoslices of ZY1709_15, showing internal diagenetic structures.

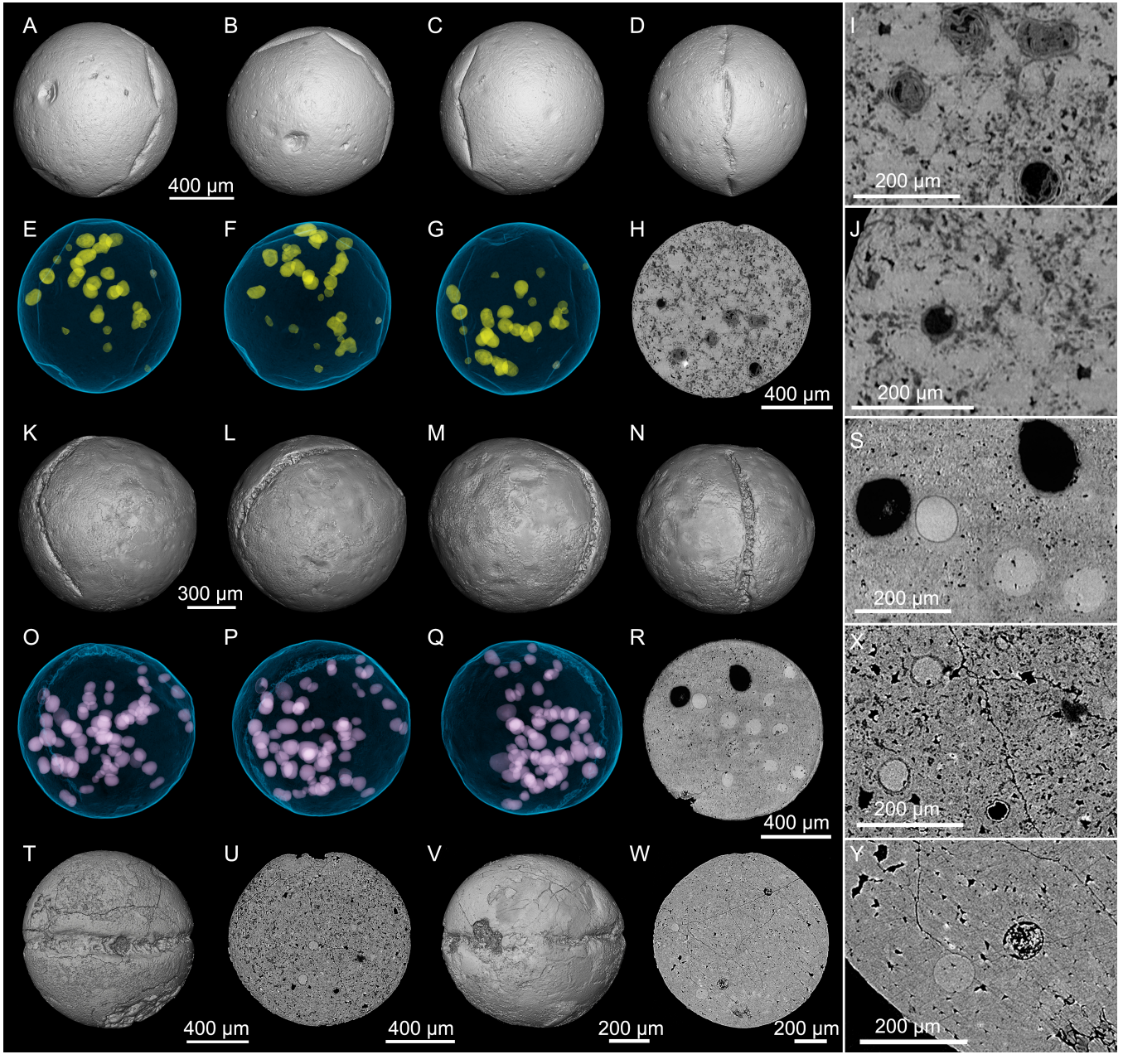
A
B
C
D
400 µm
E
F
G
H
400 µm
K
L
M
N
300 µm
O
P
Q
R
400 µm
T
U
V
W
400 µm
400 µm
200 µm
200 µm
I
200 µm
J
200 µm
S
200 µm
X
200 µm
Y
200 µm

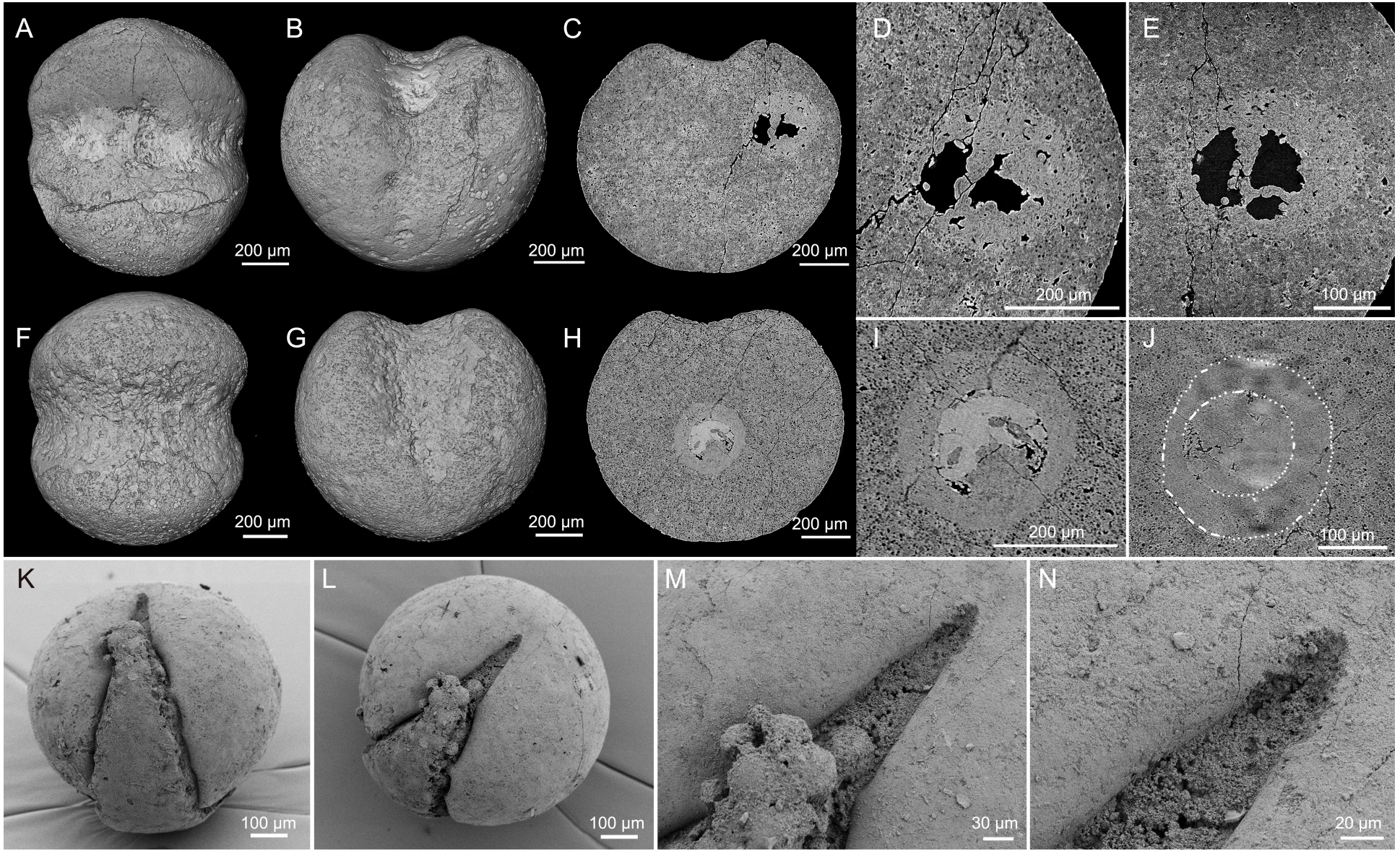
A
200 µm
B
200 µm
C
200 µm
D
200 µm
E
100 µm
F
200 µm
G
200 µm
H
200 µm
I
200 µm
J
100 µm
K
100 µm
L
100 µm
M
30 µm
N
20 µm

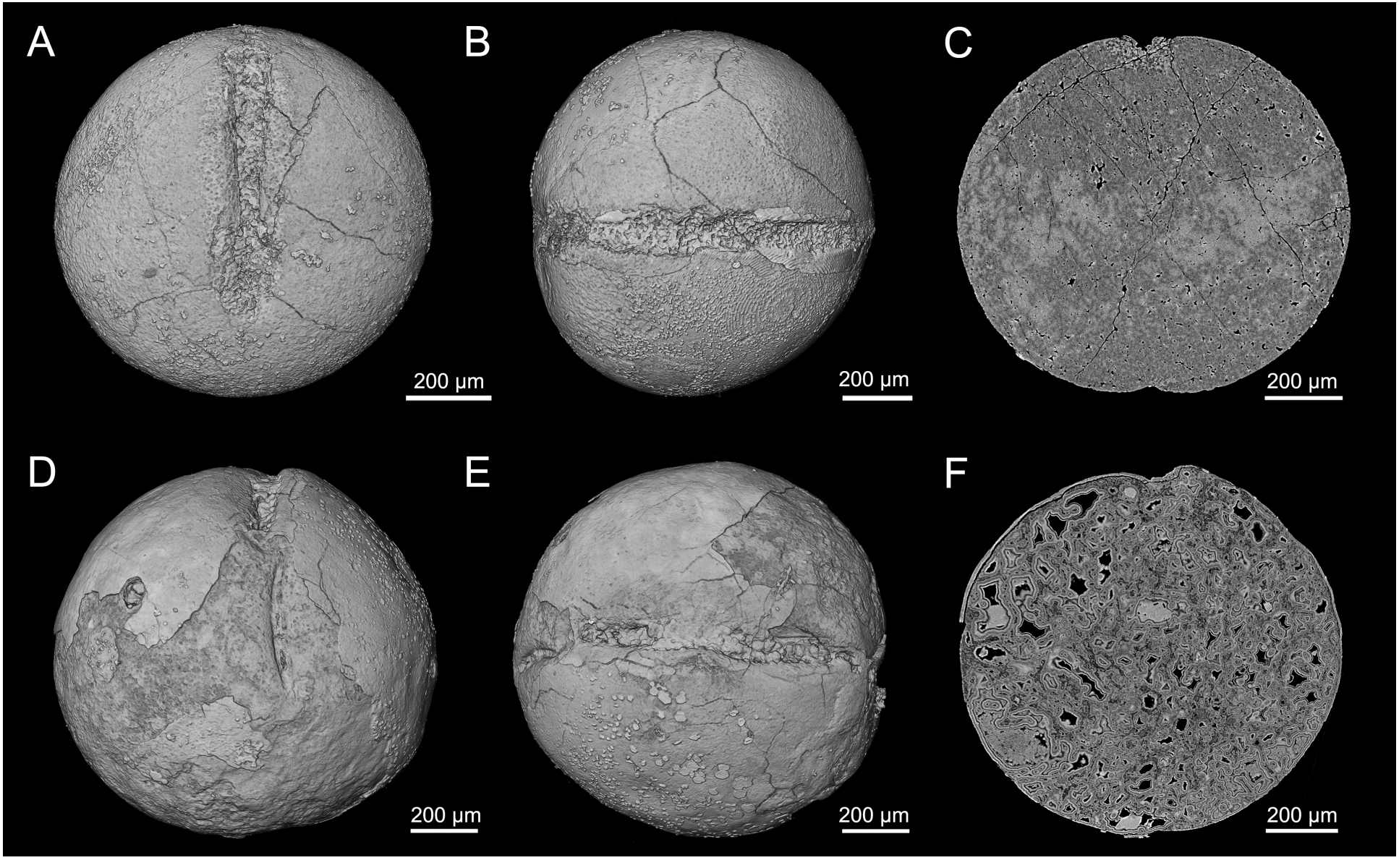
A
200 µm
B
200 µm
C
200 µm
D
200 µm
E
200 µm
F
200 µm